PIEZO1-mediated mechanosensing governs NK cell killing efficiency in 3D

Archana K. Yanamandra[1,2], Jingnan Zhang[2], Galia Montalvo[1,4,5], Doreen Biedenweg[3], Markus Hoth[1], Franziska Lautenschläger[4,5], Oliver Otto[3], Aránzazu del Campo[2,6], Bin Qu[1]

[1] Biophysics, Center for Integrative Physiology and Molecular Medicine (CIPMM), School of Medicine, Saarland University, Homburg, Germany

[2] INM - Leibniz Institute for New Materials, Saarbrücken, Germany

[3] Institute of Physics, University of Greifswald, Greifswald, Germany

[4] Department of Experimental Physics, Saarland University, Saarbrücken, Germany

[5] Center for Biophysics, Saarland University, Saarbrücken, Germany

[6] Chemistry Department, Saarland University, Saarbrücken, Germany

Corresponding author

Bin Qu

Biophysics, Center for Integrative Physiology and Molecular Medicine (CIPMM)
School of Medicine, Saarland University, 66421 Homburg, Germany.
Tel: +49 6841 16 16310, Fax: +49 6841 16 16302
Email: bin.qu@uks.eu

Abstract

Natural killer (NK) cells play a vital role in eliminating tumorigenic cells. Efficient locating and killing of target cells in complex three-dimensional (3D) environments is critical for their functions under physiological conditions. Recent studies have shown that NK cell activation is regulated by substrate stiffness. However, the role of mechanosensing in regulating NK cell killing efficiency in physiologically relevant scenarios is poorly understood. In this study, we report that the responsiveness of NK cells is regulated by tumor cell stiffness. NK cell killing efficiency in 3D is impaired against softened tumor cells, while it is enhanced against stiffened tumor cells. Notably, the durations required for NK cell killing and detachment are significantly shortened for stiffened tumor cells. Furthermore, we have identified PIEZO1 as the predominantly expressed mechanosensitive ion channel in NK cells. Perturbation of PIEZO1 by GsMTx4 abolishes stiffness-dependent NK cell responsiveness, significantly impairs the killing efficiency of NK cells in 3D, and substantially reduces NK cell infiltration into 3D collagen matrices. Conversely, PIEZO1 activation enhances NK killing efficiency as well as infiltration. In conclusion, our findings demonstrate that PIEZO1-mediated mechanosensing is crucial for NK killing functions, highlighting the role of mechanosensing in NK cell killing efficiency under physiological conditions and the influence of environmental physical cues on NK cell functions.

Significance Statement

This study reports that NK cell responsiveness is regulated by tumor cell stiffness, with impaired killing against softened tumor cells and enhanced killing against stiffened ones. PIEZO1 is the predominantly expressed mechanosensitive ion channel in NK cells, and it plays a crucial role in regulating NK infiltration into collagen matrices, which in turn affects their killing efficiency in 3D. These findings highlight the importance of mechanosensing in NK cell functions under physiological conditions.

Introduction

Natural killer (NK) cells are a crucial arm in the innate immune system, responsible for eliminating aberrant cells such as tumorigenic cells and pathogen-infected cells. In both physiological and pathological conditions, NK cells must navigate through three-dimensional (3D) environments to locate their target cells. NK cells identify the cognate target cells through the engagement of their activating receptors with ligands on the target cell surface and/or detection of absence of self-molecules using their inhibitory receptors (1). Upon target cell recognition, NK cells form an intimate contact termed the immunological synapse (IS) and reorient the killing machineries towards target cells (2). The primary killing mechanism employed by NK cells is lytic granules containing cytotoxic proteins such as pore-forming protein perforin and serine protease granzymes. Lytic granules are enriched and released at the IS to induce apoptosis or direct lysis of target cells (3). Degranulation, or the release of lytic granules, is a hall mark of NK activation triggered by target cell recognition.

Stiffness is a physical characteristic that can differ significantly between healthy and diseased tissues. For instance, solid tumors are often stiffer than the neighboring healthy tissues primarily due to a highly compacted extracellular matrix (4). Conversely, malignant cells with a high potential for metastasis are typically softer than their counterparts (5, 6). Despite the extensive research on the functional role of chemical cues, the impact of stiffness on functions of immune killer cells, especially in killing-related processes, has only recently gained attention. For NK cells, stiffer substrates potentiate polarization of MTOC, enrichment and release of lytic granules, cytokine production, and the stability of the IS (7). In addition, the actin retrograde flow at the IS, which regulates the NK cell response, is influenced by substrate stiffness (8). The stiffness of cancer cells typically ranges from a few hundred to a few thousand Pa (9-13). The ‘stiff’ substrate stiffness used to investigate the stiffness-regulated NK cell function is often two to three orders of magnitude higher than the actual stiffness of cancer cells. Therefore, the

precise effect of the physiological range of tumor cell stiffness on the effector functions and the corresponding killing efficiency of NK cells remains unclear.

To detect environmental stiffness, cells rely on mechanosensing through surface mechanosensors, mainly mechanically activated ion channels (14). In this regard, the PIEZO family is the most extensively studied mechanosensors. In T cells, PIEZO1-mediated mechanosensing of fluid shear stress has been found to potentiate T cell activation (15). Additionally, PIEZO1 activation at the IS is essential for optimal T cell receptor signal transduction, potentially through PIEZO1-mediated Ca^{2+} influx (16). In mice, genetic deletion of PIEZO1 in T cells selectively expand Treg population and attenuates the severity of experimental autoimmune encephalomyelitis, an animal model for multiple sclerosis (17). In myeloid cells, PIEZO1-mediated mechanosensing of cyclical pressure, as experienced in lungs, plays a key role in the initiation of proinflammatory response elicited by macrophages and monocytes (18). However, the functional roles of PIEZOs in NK cells have yet to be characterized.

In this study, we show that the efficiency of NK cell-mediated target cell elimination is regulated by the stiffness of target cells. Specifically, the cytotoxicity of NK cells is decreased against softer target cells and elevated against stiffer target cells. In human NK cells, mechanosensing is primarily mediated by PIEZO1, and perturbation of PIEZO1 abolishes stiffness-dependent responsiveness of NK cells. Furthermore, PIEZO1-mediated mechanosensing governs the infiltration of NK cells into 3D collagen matrices, significantly impacting NK cell killing efficiency in 3D scenarios. In summary, our results highlight the critical regulatory roles of mechanosensing in NK cell-mediated target cell elimination in physiologically relevant 3D scenarios.

Materials and Methods

Antibodies and reagents

The following antibodies were purchased from BioLegend: PerCP anti-human CD3, BV421 anti-human CD3, APC anti-human CD56, BV421 anti-human CD107a, Biotin anti-human NKp46 (CD335), Biotin Mouse IgG1-κ Isotype, BV421 anti-human Perforin, PE anti-human Perforin, and PE anti-human Granzyme B. Calcein-AM and Carboxyfluorescein succinimidyl ester (CFSE) were purchased from Thermo Fischer Scientific, GsMTx4 from Smartox Biotechnology, Blebbistatin from Cayman Chemical, Yoda-1 from Tocris, and Fibricol Collagen solution (10mg/ml Bovine Type I) from Advanced Biomatrix.

Cell culture

Human peripheral blood mononuclear cells (PBMCs) of healthy donors were isolated from Leucocyte Reduction System Chamber using a gradient centrifugation method with Lymphocyte Separation Medium 1077 (PromoCell). Primary NK cells were isolated from the PBMCs using human NK cell isolation kit (Miltenyi) and then cultured in AIM V media with 10% FCS in presence of recombinant human IL-2 (100 U/ml, Miltenyi) for 3 days, unless mentioned otherwise.

As for K562 cells and K562-pCasper cells, they were cultured in RPMI medium supplemented with 10% FCS and 1 % penicillin and streptomycin (Thermo Fischer Scientific). For K562-pCasper cells, which stably express a FRET based apoptosis reporter (19), the culture medium was additionally supplemented with puromycin (0.2 µg/ml) (VWR).

Preparation and biofunctionalization of hydrogels

Poly (acrylamide-co-acrylic acid) (PAAm-co-AA) hydrogels of varying stiffness were prepared and functionalized as previously described (20). Briefly, AAm monomer and bis-AAm crosslinker were mixed in different ratios, with a constant ratio of AA for biofunctionalization. Hydrogel discs were prepared between two coverslips. One coverslip (diameter 25 mm, VWR) was functionalized with 3-APS for covalent binding to the PAAm-co-AA hydrogel, while the other coverslip (diameter 13 mm, VWR) was coated with Sigmacote® to avoid hydrogel sticking. Glass coverslips were cleaned with ethanol and plasma before use. The degassed monomer solution, the initiator APS (10% solution, 1/100 of total volume) and TEMED (catalyst, 1/1000 of total volume) were mixed and 8 –12 μL of this mixed solution was quickly placed on 3-APS-functionalized 25 mm coverslips and covered with Sigmacote®-coated 13 mm coverslips for 10 min at RT. The sandwich-like substrate was then immersed in PBS overnight and the 13 mm coverslips were removed. The hydrogel discs were stably fixed to the glass coverslips throughout the experiments. Functionalized hydrogels of varying stiffness were incubated with streptavidin solution (100 μg/mL) for 1 –1.5 h (2 kPa) or 2.5 –3 h (12 and 50 kPa) to obtain equal anti-NKp46 densities. Streptavidin-functionalized hydrogels were then incubated with biotinylated anti-NKp46 (100 μg/mL, 100 μL) or IgG isotype (100 μg/mL, 100 μL) overnight at 4°C.

CD107a Degranulation assay

To assess stimulation-induced NK degranulation, NK cells were either settled on substrates functionalized with NKp46 antibody or incubated with K562 cells in presence of BV421 anti-CD107a antibody and protein transport inhibitor Golgi stop (BD Biosciences) at 37°C with 5%

CO_2 for 4 hours. Then the cell suspension was stained with PerCP anti-human CD3, APC anti-human CD56 antibodies at 4°C in dark for 30 minutes. The samples were analyzed using FACSVerse (BD Biosciences). The $CD3^-CD56^+$ population was gated for NK cells. FlowJo v10 (FLOWOJO, LLC) was used for data analysis.

Determination of NK cell killing kinetics in 3D collagen matrices

The 3D killing assay was conducted as described previously (21). Briefly, K562-pCasper target cells were resuspend in neutralized bovine collagen I (2 mg/ml) and plated in a black 96-well plate with flat clear bottom (Corning/Merck) at a density of 25,000 cells/40 µl per well. The plate was centrifuged to spin down the target cells on the bottom and then polymerized at 37°C with 5 % CO_2 for 1 hour. NK cells were added on the top of the collagen matrix with an E:T ratio of 5:1 if not otherwise specified. A high content imaging system ImageXpress (Molecular Devices) was used to acquire images at 37°C with 5 % CO_2 every 20 minutes for 48 hours. K562-pCasper target cells with a FRET signal above the threshold (maximal FRET signals in GFP-positive target cells) were taken as live target cells. The number of live target cells at each time point was normalized to that at time 0. AIMV medium supplemented with 10% FCS was used in this assay. The images were processed and analyzed using ImageJ.

NK cell migration in 3D collagen matrices

NK cells were stained with CFSE (5 µM in PBS/4.5% FCS) at room temperature for 15 minutes, washed once with PBS, then resuspended in AIMV/10% FCS and kept at 37°C with 5 % CO_2 overnight for recovery. Sample preparation for light-sheet microscopy was describe previously (22). Briefly, CFSE-stained NK cells were resuspended in neutralized bovine collagen I (2

mg/ml), and this cell suspension was polymerized in a capillary at 37°C with 5 % CO_2 for 1 hour. Subsequently, the sample was mounted in the sample chamber filled with RPMI medium. Z-stacks (step size ~ 2 µm for ~ 100 slices) were acquired using a Z.1 light-sheet microscope (Zeiss) at 37°C every 30 seconds for 30 minutes. Imaris 8.1.2 (Bitplane) was used to automatically track fluorescently labeled NK cells to quantify cell velocity and persistence.

Analysis of NK cell infiltration into 3D collagen matrices

NK cells were stained with CFSE (5 µM in PBS/4.5% FCS) at room temperature for 15 minutes, washed once with PBS, then resuspended in AIMV/10% FCS and kept at 37°C with 5 % CO_2 overnight for recovery. Neutralized bovine collagen I (2 mg/ml) was plated 40 µl per well in a black 96-well plate with flat clear bottom (Corning/Merck). The plate was kept at 37°C with 5 % CO_2 for 1 hour. After solidification, CFSE-stained NK cells (125,000 cells/well) were added on the top of the matrix. To identify the position of the bottom, one well plated with NK cells without collagen was used as reference. Images focused on the bottom were acquired using ImageXpress at 37°C with 5 % CO_2 every 20 minutes for 48 hours. ImageJ was used to identify fluorescently labeled NK cells and quantify the number of infiltrated NK cells for each time point.

Determination of cytotoxic protein expression

NK cells were washed twice with PBS containing 0.5% BSA, then stained with PerCP anti-human CD3, APC anti-human CD56 antibodies at 4°C in dark for 30 minutes. To assess the expression of perforin and granzyme B, these pre-stained NK cells were fixed with pre-chilled 4 % paraformaldehyde (PFA) for 15 minutes, permeabilized with PBS containing 0.1%

saponin, 0.5% BSA, and 5% FCS at room temperature for 15 minutes, then stained with BV421 anti-human Perforin and PE anti-human Granzyme B antibodies at 4°C in dark for 30 minutes. The samples were analyzed using FACSVerse (BD Biosciences). The $CD3^{-}CD56^{+}$ population was gated for NK cells. FlowJo v10 (FLOWOJO, LLC) was used for data analysis.

Ethical considerations

Research carried out for this study with material from healthy donors (Leukocyte Reduction System Chambers from human blood donors) has been authorized by the local ethic committee Ethik-Kommission bei der Ärztekammer des Saarlandes (Identification Nr. 84/15, Prof. Dr. Rettig-Stürmer).

Statistical analysis

GraphPad Prism 9 Software (GraphPad) was used for statistical analysis. For un-paired groups, Mann-Whitney-U-test was used. For paired groups, Wilcoxon matched-pairs signed rank test was used.

Results

NK cell activation is regulated by surface stiffness

To investigate how the stiffness of target cells affects NK cell responsiveness, we used functionalized hydrogels of various stiffness as a model system to mimic target cells (20). Specifically, we employed poly (acrylamide-co-acrylic acid) (PAAm-co-AA) hydrogels with Young's Modulus of 2, 12, and 50 kPa, which were functionalized with biotin-PEG 8-NH 2 and subsequently incubated with streptavidin (Fig. 1A). To activate NK cells, we coated the streptavidin-functionalized hydrogels with biotinylated activating antibody targeting NKp46 (Fig. 1A), which belongs to the natural cytotoxicity receptor family. We used NK cells that were isolated from healthy donors and stimulated with IL-2 for 3 days. To evaluate NK activation, we settled NK cells on the functionalized hydrogels at 37°C for four hours and assessed degranulation of lytic granules based on the levels of CD107a on the surface of the NK cells. CD107a is exclusively expressed on vesicular membrane of lytic granules and can only be integrated into the plasma membrane of NK cells after lytic granule release (23). Based on activation-triggered degranulation, we found that NK cells fell into four categories: only activated on 50 kPa (5 out of 12, Fig. 1B), only activated on 12 kPa (3 out of 12, Fig. 1C), activated on all three stiffness levels (2 out of 12, Fig. 1D), or no response (2 out of 12, Fig. 1E). Importantly, degranulation was only triggered by activation of NKp46, as isotype IgG-coated hydrogels did not induce degranulation (Fig. 1B-D, isotype). Notably, NK cells from most donors (10 out of 12) did not respond to very soft hydrogels (2 kPa) (Fig. 1F, G). These findings show that NK cells cannot be fully activated on soft substrates, which is consistent with previous reports (7, 8). Based on these results, we hypothesized that softening target cells would impair NK killing capacity.

Target cell stiffness modulates NK cell cytotoxicity

To test our hypothesis, we softened the target cells (K562 cells) by DMSO treatment as determined by real-time deformability cytometry (RT-DC) (Fig. 2A). The K562 cells used in

our study stably express a FRET-based apoptosis reporter pCasper (K562-pCasper), consisting of a GFP and RFP pair linked by a caspase recognition site (DEVD) (19). Upon initiation of apoptosis, the orange-colored target cells lose their FRET signal and turn green. In the case of necrosis, fluorescent proteins would leak out of the destructed plasma membrane, resulting in the complete loss of fluorescence. To evaluate NK cell killing efficiency in a 3D environment, we embedded K562-pCasper target cells in bovine type I collagen and added IL-2-stimulated primary human NK cells from the top after solidification. This setup allows NK cells to infiltrate the collagen matrix and search for their target cells in a physiologically relevant scenario. We monitored killing events at 37°C every 20 minutes for 48 hours were visualized using a high content imaging system. Our results show that the killing efficiency of NK cells against DMSO-treated target cells was reduced compared to that against untreated cells (Fig. 2B, Supplementary Movie 1). These findings suggest that softening of tumor cells weakens NK cell killing capacity.

Next, we examined whether increasing the stiffness of tumor cells could have the opposite effect. To do this, we used blebbistatin, a myosin IIA inhibitor known to enhance the stiffness of cells in suspension by perturbing actomyosin contractility (24). Our analysis of RT-DC revealed that blebbistatin treatment reduced the deformability of target cells, indicating an increase in their stiffness relative to vehicle-treated control cells (Fig. 2C). Interestingly, we observed an elevated killing efficiency of NK cells against the stiffened blebbistatin-treated tumor cells (Fig. 2D, Supplementary Movie 2). Notably, analysis of live cell imaging showed a significant reduction in the time required for NK killing (i.e. duration from contact to apoptosis) and the total contact time between NK and target cells (i.e. duration from contact till detachment) in the case of stiffened tumor cells compared to the control group (Fig. 2E, F). Together, these results suggest that the stiffness of target cells has a significant impact on the outcome of NK killing efficiency.

PIEZO1 mediates NK cell responsiveness to target cell stiffness

Mechano-sensing is crucial for cells to detect stiffness of surrounding environment and the cells they encounter. Among the mechanosensitive channels, PIEZO1 is the most predominantly expressed in primary human NK cells (Fig. 3A). However, down-regulating PIEZO1 in primary human NK cells is technically challenging. Therefore, to examine the functional role of PIEZO1 in stiffness-regulated NK activation, we used GsMTx4, a peptide isolated from spider venom that inhibits the mechanosensitivity of PIEZO1 (25). Our results showed that the surface stiffness-dependent degranulation of NK cells was completely abolished by GsMTx4 treatment (Fig. 3B). Specifically, in GsMTx4-treaed NK cells, activation-triggered degranulation was elevated on soft surfaces (2 kPa) but substantially decreased on stiffer surfaces (12 and 50 kPa) (Fig. 3B), indicating that PIEZO1 plays a pivotal role in mediating mechano-sensing in NK cells.

To investigate the effects of PIEZO1 perturbation on NK cell killing function, we further evaluated NK cell killing in a 3D scenario. Results from the 3D killing assay showed that GsMTx4-treated NK cells almost entirely lost their ability to kill target cells in 3D (Fig. 3C, Supplementary Movie 3). To explore the underlying mechanisms, we examined the lytic granule pathway and NK cell migration. We found that GsMTx4 treatment did not alter the expression of cytotoxic proteins such as perforin and granzyme B (Fig. 3D). Furthermore, degranulation induced by target cell recognition was even slightly enhanced (Fig. 3E). Notably, the numbers of NK cells that infiltrated the 3D collagen matrix were greatly reduced after GsMTx4 treatment (Fig. 3F). These observations suggest that PIEZO1-mediated mechno-sensing is crucial for NK cells to execute their killing function in 3D mainly by regulating of NK infiltration into the 3D matrix.

Aside from PIEZO1, GsMTx4 also targets a few other mechanically activated ion channels such as TRPC1, TRPC6 and TACAN. Although the expression levels of TRPC1, TRPC6 and TACAN are very low, if not negligible, compared to PIEZO1 (Fig. 3A), to confirm the effect of PIEZO1, we utilized a PIEZO1 specific agonist, Yoda-1. Indeed, Yoda-1-treated NK cells

exhibited an acceleration in killing kinetics (Fig. 4A, Supplementary Movie 4). Yoda-1-treated NK cells exhibited shortened time to initiate killing compared to the control group (Fig. 4B). No difference was observed in degranulation induced by target cell recognition (Fig. 4C), or in the conjugation between NK cells and target cells (Fig. 4D) by in Yoda-1-treated NK cells. Interestingly, infiltration of NK cells into 3D collagen matrix was substantially accelerated by Yoda-1 treatment (Fig. 4E-F, Supplementary Movie 5). Vehicle-treated NK cells first appeared in the focal plane at 6.6±1.6 hours, whereas first Yoda-1-treated NK cells approached the focal plane at around 4.8±1.7 hours (Fig. 4F). Taken together, our results suggest that PIEZO1 functions as the primary mechanosensor to regulate NK killing efficiency, especially in 3D environments.

Discussion

In our study, we have demonstrated that the final killing efficiency of NK cells can be modulated by manipulating the stiffness of target cells. Cell softening is a recently discovered characteristic of malignant tumor cells, which is associated with tumorigenicity and malignancy. A rich body of evidence proves that cancer cells are softer than their non-malignant normal counterparts (26). For example, ovarian cancer cells have a Young's modulus in the range of 0.5-1 kPa, whereas their non-malignant counterpart have a stiffness of around 2 kPa, as determined by atomic force microscopy (AFM) (9). Similarly, cervical cancer cells (Hela cells) have an elastic modulus of ~2 kPa, which is lower than that of normal human cervix epithelial cells (End1/E6E7 cells, elastic modulus E ~4-5 kPa) (10). Notably, even among malignant cells, the stiffness can vary, and softer cancer cells exhibit enhanced tumorigenicity, metastasis, and stemness. For example, among two ovarian cancer cell lines from the same specimen, the soft cells (HEY A8, ~0.5 kPa) are more invasive than their stiffer counterparts (HEY, ~0.9 kPa) (9). Soft cancer cells (breast cancer and melanoma cells, ~0.2-0.3 kPa) require only ten cells to generate metastatic tumors in the lungs, whereas even 100 stiff cancer cells (~0.8-1 kPa) are unable to produce any detectable lung metastasis (12). Softer cancer cells not only form more colonies with bigger sizes *in vitro*, but also have a substantially higher frequency of forming tumors *in vivo* (12). Stemness-associated genes are also up-regulated in soft tumor cells (12). Additionally, a study using cancer organoids embedded in 3D collagen has shown that cancer cells at the peripheral region are softer than the cells in the core region, and softer cancer cells are more invasive and metastatic (13). Tumor cells can be further softened by migration through confined spaces (13). In our study, the stiffness of non-treated tumor cells (~1 kPa), softened tumor cells (~0.6-0.7 kPa), or stiffened tumor cells (~1.2-1.4 kPa) falls within the range of physiological stiffness as reported in the aforementioned studies. Our results demonstrate that softening (or stiffening) tumor cells substantially reduces (or enhances) elimination by NK cells,

providing direct evidence supporting the hypothesis that cell softening is a mechanism by which malignant cells evade immune surveillance.

How does softening or stiffening of tumor cells affect the cytotoxicity of NK cells? In the process of cell killing, several key steps are critical, such as the initiation of IS formation, lytic granule enrichment and release, cytotoxic protein uptake by target cells, and detachment of NK cells after killing. Our study shows that softening or stiffening of tumor cells does not significantly alter lytic granule release, indicating that the events upstream of lytic granule release, such as IS formation and lytic granule enrichment, are unlikely to be significantly affected. However, we observed that the duration required to induce apoptosis or necrosis of tumor cells is prolonged for softened tumor cells compared to their stiff counterpart. Perforin-mediated pore formation on the plasma membrane of target cells is a critical step for directly lysing target cells or facilitating granzyme entry into target cells to induce apoptosis. Reduced tension of target cells impairs perforin-mediated pore formation and perforin-dependent killing (27). Therefore, to kill softened tumor cells, NK cells likely need to release more perforin or require more time to form the pores. Both scenarios require a longer duration for the killing process.

Following a successful killing, NK cells must detach from the dying or dead target cells in a timely manner to search for other targets and carry out more killing. Intriguingly, our observations show that the duration from the initiation of target cell apoptosis to the detachment of NK cells from stiffened target cells is substantially shorter than that from their softer counterparts. This finding suggests that alteration in tumor cell stiffness may influence the process of NK cell detachment. The mechanisms that regulate NK cell detachment from target cells remain largely elusive, despite one study has been shown that conjugation with newly identified target cells can accelerate NK cell detachment from old target cells (28). Nevertheless, studies on cytotoxic T lymphocytes suggest that recovery of cortical actin at the IS is essential to terminate lytic granule secretion, suggestively enabling or promoting T cells to detach from

their target cells (29). PKCθ is required to break the symmetry of the IS, allowing naive T cells to disengage from their target cells (30). Additionally, calcium influx also contributes to T cell disengagement from a target cell (31). Therefore, it is possible that NK cells employ similar mechanisms to terminate killing processes and disassemble the IS, which is necessary for detachment from target cells. Interestingly, cell stiffness changes or increases after cell death (32, 33), which can serve as a direct cue to initiate NK cell detachment.

Recent studies have revealed that mechanical cues, particularly stiffness, can regulate the functions of NK cells. When primary human NK cells are stimulated with IL-2 on MICA-functionalized substrate with varying stiffness (30, 150, and 3000 kPa), they exhibit a bell-shaped response, with the maximum degranulation and clustering of DAP10 (an adaptor molecule downstream of NKG2D) occurring at 150 kPa (34). The application of mechanical forces to NK cells via MICA-functionalized nanowires (diameter ~ 50 nm) enhances lytic granule degranulation upon NKG2D activation (35). Similarly, stiffer sodium alginate beads (34 and 254 kPa) functionalized with NKp30 antibody can induce full NK cell activation characterized by MTOC translocation and lytic granule polarization, whereas softer beads (9 kPa) failed to do so (7). Our data also suggest that NK cells exhibit greater degranulation triggered by activating receptors on stiffer hydrogels (12 and 50 kPa) compared to soft hydrogels (2 kPa) for most donors. However, for some donors, the levels of degranulation were comparable across all three stiffness levels. These findings indicate that NK cell responsiveness to stiffness is donor-dependent and could be attributed to differences in the expression of mechanosensors and/or downstream effector molecules.

Mechanical cues are detected by various professional mechanosensors, primarily mechanosensitive ion channel families, among which are the PIEZO family, TREK/TRAAK K2P (two-pore potassium) channels, TMEM63 (hyperosmolality-gated calcium-permeable) channels, and TMC (Transmembrane channel-like) 1/2 (14, 36). In our study, we report that PIEZO1 is the predominant mechanosensitive channel expressed in NK cells, indicating its

indispensable role in mechanotransduction in NK cells. WE observed that inhibiting PIEZO1 using GsMTx4 nearly abolished NK cell responsiveness to different substrate stiffness, greatly impaired NK cell-mediated cytotoxicity, and substantially reduced NK cell infiltration into 3D collagen matrices. Conversely, activating PIEZO1 with Yoda-1 enhanced the killing efficiency and infiltration capacity of NK cells. These findings demonstrate that PIEZO1-mediated mechanosensing is crucial for NK killing functions, highlighting PIEZO1 as a promising target to modulate NK functions, particularly in the context of solid tumors.

Conflict of Interest

The authors declare that the research was conducted in the absence of any commercial or financial relationships that could be construed as a potential conflict of interest.

Author Contributions

AKY performed most of the experiments and the corresponding analysis if not mentioned otherwise; JZ prepared hydrogels; GM, FL, DB, and OO helped with RT-DC, MH and AdC helped with data interpretation and provided critical feedback on all aspects of the project; BQ generated concepts and designed experiments; All authors contributed to the writing, editing and cross-checking of the manuscript.

Acknowledgments

We thank the Institute for Clinical Hemostaseology and Transfusion Medicine for providing donor blood, Carmen Hässig, Cora Hoxha, Gertrud Schäfer, Kathrin Förderer for excellent technical help; This project was funded by the Deutsche Forschungsgemeinschaft (SFB 1027 Project A2 to BQ, A10 to FL, A11 to MH, B6 to AdC, and GZ: INST 256/419-1 FUGG).

Ethical considerations

Research carried out for this study with material from healthy donors (leukocyte reduction system chambers from human blood donors) is authorized by the local ethic committee Ethik-Kommission bei der Ärztekammer des Saarlandes (Identification Nr. 84/15, Prof. Dr. Rettig-Stürmer).

References

1. S. Sivori *et al.*, Human NK cells: surface receptors, inhibitory checkpoints, and translational applications. *Cell Mol Immunol* **16**, 430-441 (2019).
2. J. S. Orange, Formation and function of the lytic NK-cell immunological synapse. *Nat Rev Immunol* **8**, 713-725 (2008).
3. K. Krzewski, J. E. Coligan, Human NK cell lytic granules and regulation of their exocytosis. *Front Immunol* **3**, 335 (2012).
4. M. W. Pickup, J. K. Mouw, V. M. Weaver, The extracellular matrix modulates the hallmarks of cancer. *EMBO Rep* **15**, 1243-1253 (2014).
5. C. Rianna, M. Radmacher, S. Kumar, Direct evidence that tumor cells soften when navigating confined spaces. *Mol Biol Cell* **31**, 1726-1734 (2020).
6. A. B. Roberts *et al.*, Tumor cell nuclei soften during transendothelial migration. *J Biomech* **121**, 110400 (2021).
7. D. Friedman *et al.*, Natural killer cell immune synapse formation and cytotoxicity are controlled by tension of the target interface. *J Cell Sci* **134** (2021).
8. O. Matalon *et al.*, Actin retrograde flow controls natural killer cell response by regulating the conformation state of SHP-1. *EMBO J* **37** (2018).
9. W. Xu *et al.*, Cell stiffness is a biomarker of the metastatic potential of ovarian cancer cells. *PLoS One* **7**, e46609 (2012).
10. K. Hayashi, M. Iwata, Stiffness of cancer cells measured with an AFM indentation method. *J Mech Behav Biomed Mater* **49**, 105-111 (2015).
11. Y. L. Han *et al.*, Cell swelling, softening and invasion in a three-dimensional breast cancer model. *Nat Phys* **16**, 101-108 (2020).
12. J. Lv *et al.*, Cell softness regulates tumorigenicity and stemness of cancer cells. *EMBO J* **40**, e106123 (2021).
13. C. Rianna, M. Radmacher, S. Kumar, Direct evidence that tumor cells soften when navigating confined spaces. *Molecular Biology of the Cell* **31**, 1726-1734 (2020).
14. J. M. Kefauver, A. B. Ward, A. Patapoutian, Discoveries in structure and physiology of mechanically activated ion channels. *Nature* **587**, 567-576 (2020).
15. J. M. Hope *et al.*, Fluid shear stress enhances T cell activation through Piezo1. *BMC Biol* **20**, 61 (2022).
16. C. S. C. Liu *et al.*, Cutting Edge: Piezo1 Mechanosensors Optimize Human T Cell Activation. *J Immunol* **200**, 1255-1260 (2018).
17. A. Jairaman *et al.*, Piezo1 channels restrain regulatory T cells but are dispensable for effector CD4(+) T cell responses. *Sci Adv* **7** (2021).
18. A. G. Solis *et al.*, Mechanosensation of cyclical force by PIEZO1 is essential for innate immunity. *Nature* **573**, 69-74 (2019).
19. C. S. Backes *et al.*, Natural killer cells induce distinct modes of cancer cell death: Discrimination, quantification, and modulation of apoptosis, necrosis, and mixed forms. *J Biol Chem* **293**, 16348-16363 (2018).
20. J. Zhang *et al.*, Micropatterned soft hydrogels to study the interplay of receptors and forces in T cell activation. *Acta Biomater* **119**, 234-246 (2021).
21. R. Zhao *et al.*, Targeting the Microtubule-Network Rescues CTL Killing Efficiency in Dense 3D Matrices. *Front Immunol* **12**, 729820 (2021).
22. R. Schoppmeyer, R. Zhao, M. Hoth, B. Qu, Light-sheet Microscopy for Three-dimensional Visualization of Human Immune Cells. *J Vis Exp* 10.3791/57651 (2018).
23. G. Alter, J. M. Malenfant, M. Altfeld, CD107a as a functional marker for the identification of natural killer cell activity. *J Immunol Methods* **294**, 15-22 (2004).
24. C. J. Chan *et al.*, Myosin II Activity Softens Cells in Suspension. *Biophys J* **108**, 1856-1869 (2015).

25. C. Bae, F. Sachs, P. A. Gottlieb, The mechanosensitive ion channel Piezo1 is inhibited by the peptide GsMTx4. *Biochemistry* **50**, 6295-6300 (2011).
26. C. Alibert, B. Goud, J. B. Manneville, Are cancer cells really softer than normal cells? *Biol Cell* **109**, 167-189 (2017).
27. R. Basu *et al.*, Cytotoxic T Cells Use Mechanical Force to Potentiate Target Cell Killing. *Cell* **165**, 100-110 (2016).
28. P. Netter, M. Anft, C. Watzl, Termination of the Activating NK Cell Immunological Synapse Is an Active and Regulated Process. *J Immunol* **199**, 2528-2535 (2017).
29. A. T. Ritter *et al.*, Cortical actin recovery at the immunological synapse leads to termination of lytic granule secretion in cytotoxic T lymphocytes. *Proc Natl Acad Sci U S A* **114**, E6585-E6594 (2017).
30. T. N. Sims *et al.*, Opposing effects of PKCtheta and WASp on symmetry breaking and relocation of the immunological synapse. *Cell* **129**, 773-785 (2007).
31. A. Bohineust, Z. Garcia, H. Beuneu, F. Lemaitre, P. Bousso, Termination of T cell priming relies on a phase of unresponsiveness promoting disengagement from APCs and T cell division. *J Exp Med* **215**, 1481-1492 (2018).
32. N. I. Nikolaev, T. Muller, D. J. Williams, Y. Liu, Changes in the stiffness of human mesenchymal stem cells with the progress of cell death as measured by atomic force microscopy. *J Biomech* **47**, 625-630 (2014).
33. M. Islam *et al.*, Microfluidic Sorting of Cells by Viability Based on Differences in Cell Stiffness. *Sci Rep* **7**, 1997 (2017).
34. L. Mordechay *et al.*, Mechanical Regulation of the Cytotoxic Activity of Natural Killer Cells. *ACS Biomater Sci Eng* **7**, 122-132 (2021).
35. G. Le Saux *et al.*, Nanoscale Mechanosensing of Natural Killer Cells is Revealed by Antigen-Functionalized Nanowires. *Adv Mater* **31**, e1805954 (2019).
36. D. Douguet, E. Honore, Mammalian Mechanoelectrical Transduction: Structure and Function of Force-Gated Ion Channels. *Cell* **179**, 340-354 (2019).

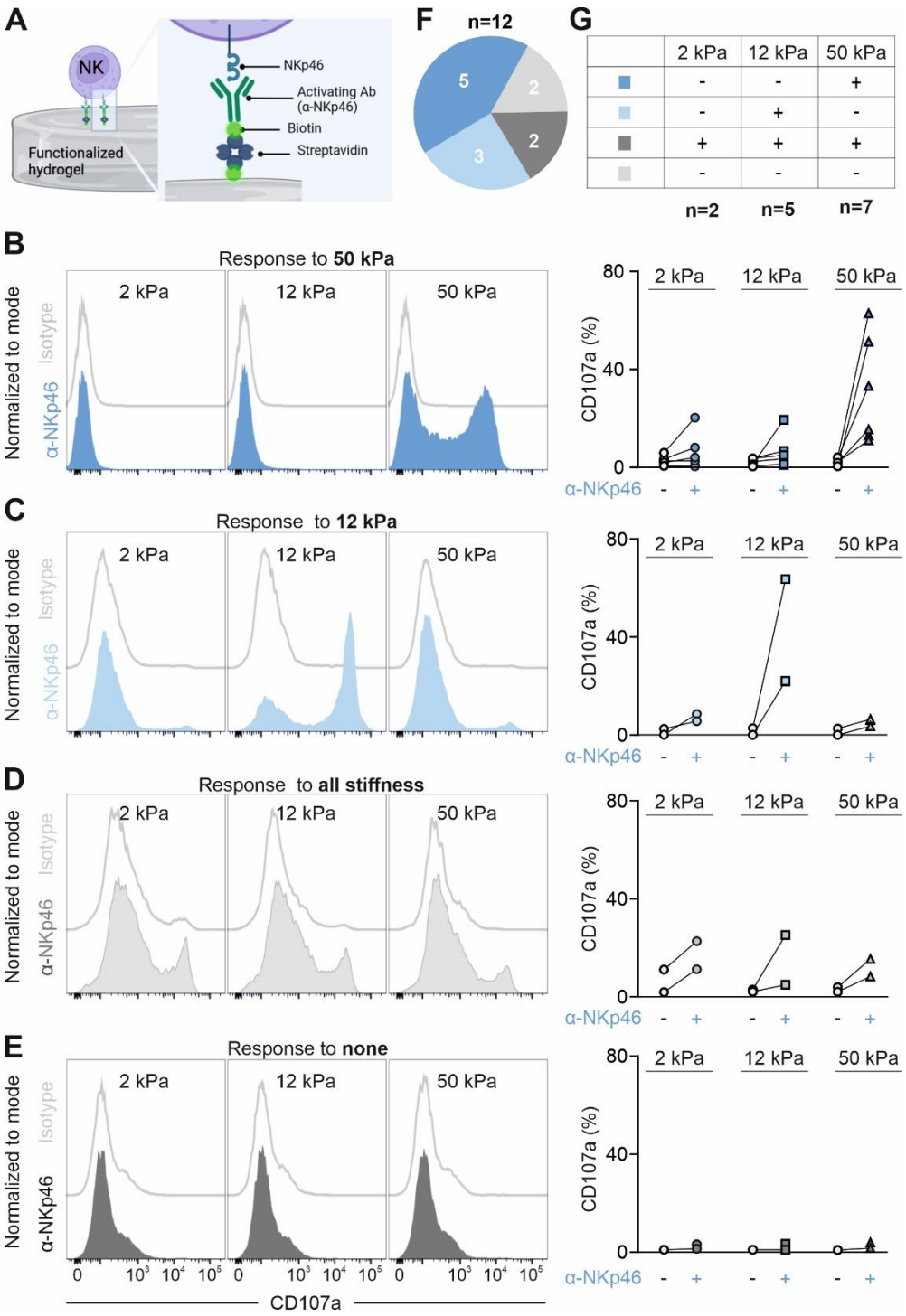

Figure 1. NK cell responsiveness to varying levels of substrate stiffness. Primary human NK cells from healthy donors were stimulated with IL-2 for three days prior to the experiments. (**A**) Sketch of functionalization of hydrogels. PAAm-co-AA hydrogels were first treated with streptavidin and then incubated with biotinylated anti-NKp46 antibodies. (**B-E**) NK cell responsiveness is substrate stiffness-dependent. The activation of NK cells was evaluated using the CD107a degranulation assay. The NK cells were settled on functionalized hydrogels at 37°C with 5% CO_2 for 4 hours in the presence of anti-CD107a antibody and Golgi Stop. The samples were then analyzed using flow cytometry. The NK cells responded to 50 kPa (**B**, n=5), 12 kPa (**C**, n=3), all stiffness levels (**D**, n=2), or did not respond to any stiffness (**E**, n=2). One representative donor is shown in the left panel and the quantification of all donors is shown in the right panel. (**F-G**) Summary of the NK cell responsiveness from different donors.

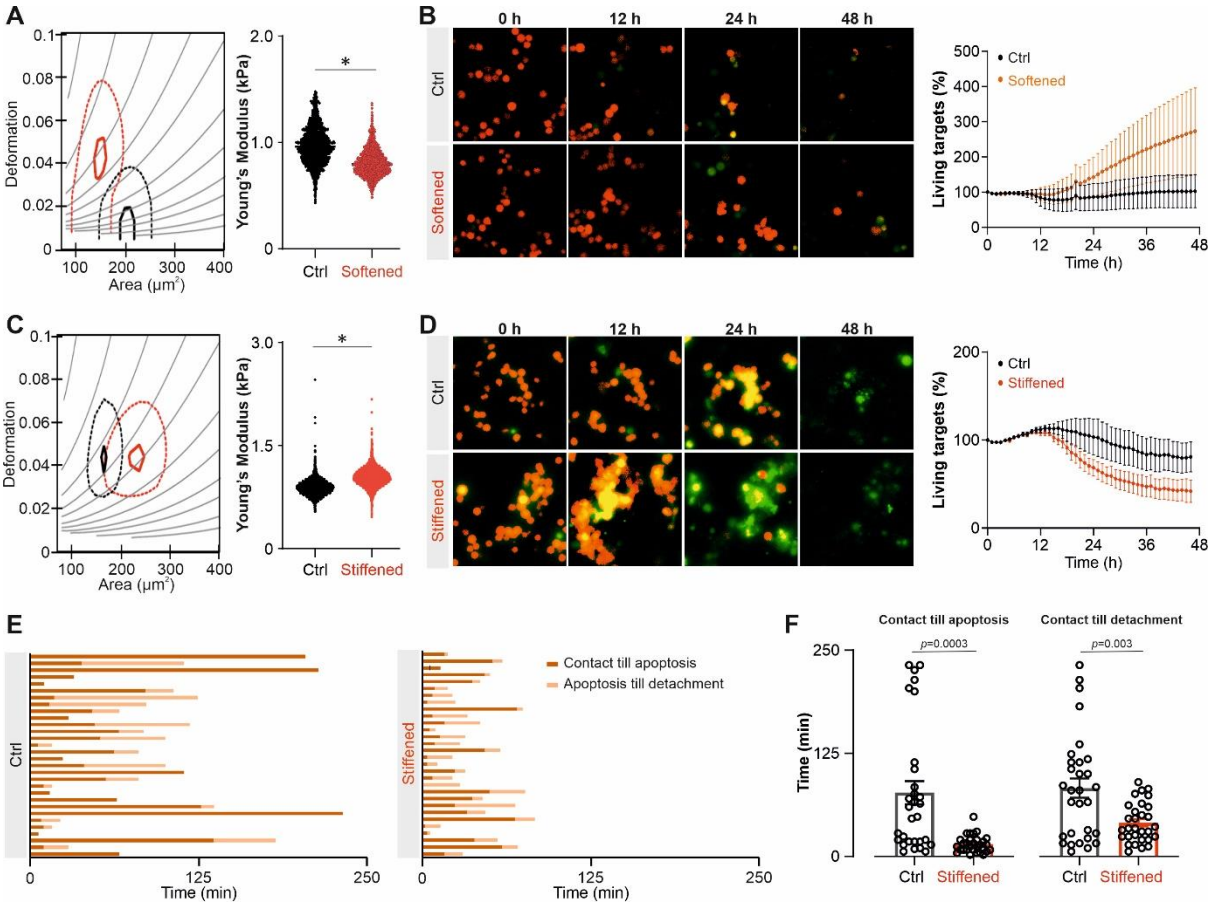

Figure 2. The killing efficiency of NK cells in 3D scenarios is regulated by tumor cell stiffness. Primary human NK cells from healthy donors were stimulated with IL-2 for three days prior to the experiments. K562-pCasper target cells were embedded in collagen matrices (2 mg/ml) and the NK cells were added from the top. Live target cells are in orange-yellow color and apoptotic target cells in green. (**A-B**) Softening tumor cells impairs NK cell killing efficiency in 3D. K562-pCasper cells were pre-treated with DMSO (Softened). Their stiffness was determined using RT-DC (**A**). Time lapse of killing events and the quantification is shown in **B**. (**C-D**) NK cells eliminate stiffened tumor cells more efficiently. K562-pCasper cells were pre-treated with Blebbistatin (Stiffened). Their stiffness was determined using RT-DC (**C**). Time lapse of killing events and the quantification is shown in **D**. (**E-F**) The duration required for NK cell killing and detachment from the stiffened tumor cells is shortened. K562-pCasper target cells were treated with DMSO (Ctrl) or Blebbistatin (Stiffened). The NK cells were co-incubated with target cells for 4 hours. The NK cells were tracked manually. The duration required for each killing event (the time from the initiation of NK/target contact to target cell apoptosis) and the duration required for NK cell detachment (the time from the initiation of NK/target contact to disengagement of NK cells from the targets) for all NK cells analyzed are shown in the left and right panel of **E**, respectively. The quantification of these durations is shown in **F**. The results were from at least three independent experiments.

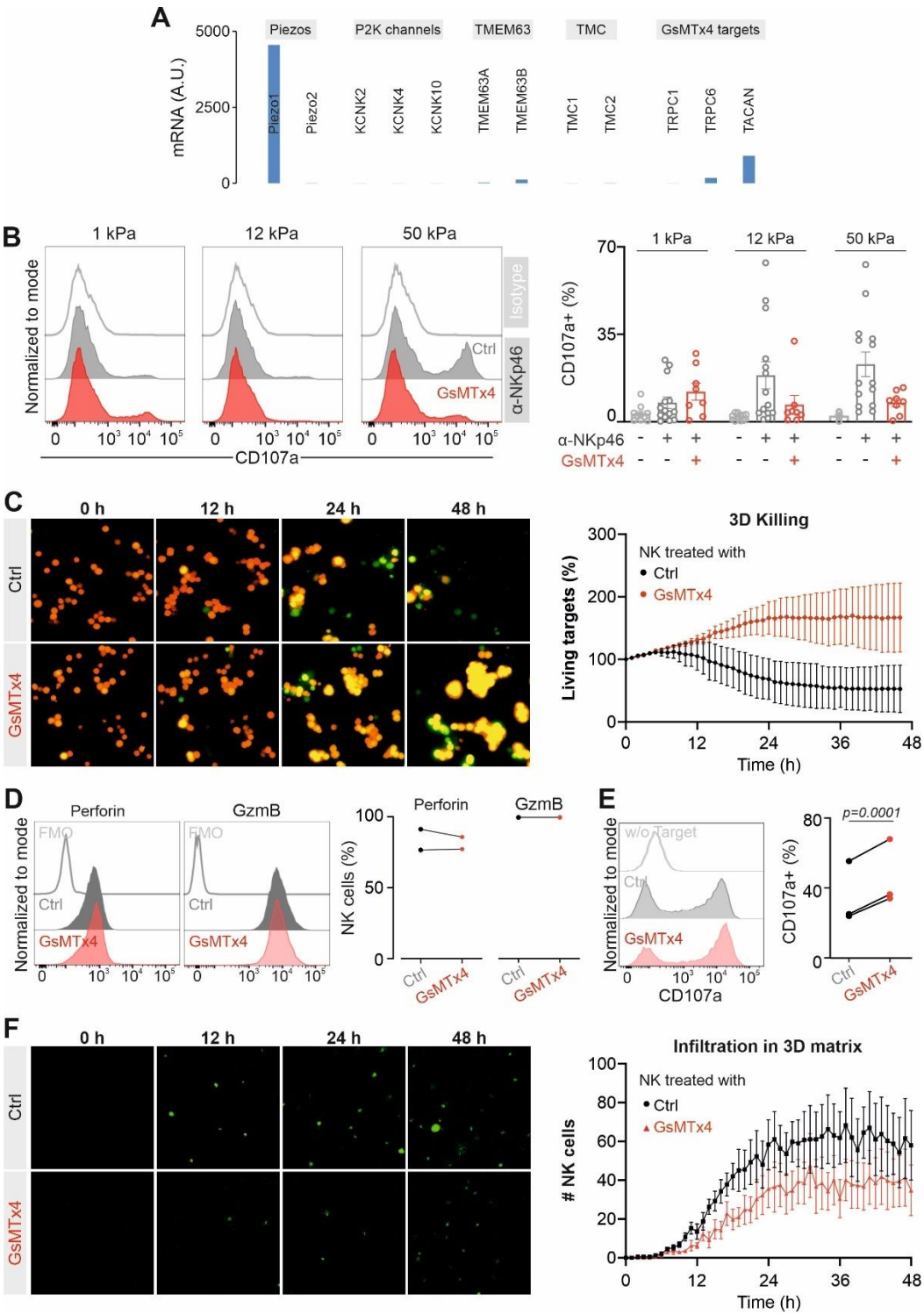

Figure 3. Inhibition of PIEZO1 reduces NK cell killing efficiency in 3D. Primary human NK cells from healthy donors were stimulated with IL-2 for three days. Prior to the experiments, the NK cells were pre-treated with GsMTx4 (10 µM) at 37°C for 30 minutes. GsMTx4 was present in the medium during the experiments. (**A**) Expression of mechanosensitive ion channels in NK cells. Expression at the mRNA level ($2^{\Delta Ct}$) was calculated based on the microarray analysis. (**B**) GsMTx4 treatment abolishes substrate stiffness-dependent NK cell responsiveness. The activation of NK cells was evaluated using the CD107a degranulation assay. One representative donor is shown in the left panel and the quantification of all donors is shown in the right panel. (**C**) The killing efficiency of GsMTx4-treated NK cells in 3D is impaired. K562-pCasper target cells were embedded in collagen matrices (2 mg/ml) and the NK cells

were added from the top. Live target cells are in orange-yellow color and apoptotic target cells in green. Time lapse of one representative donor is shown in the left panel and the quantification of all donors is shown in the right panel. (**D-E**) GsMTx4 treatment does not affect lytic granule pathway. Expression of perforin and granzyme B was assessed using flow cytometry (**D**, n=2). NK cell degranulation induced by target cell recognition was evaluated using the CD107a degranulation assay (**E**, n=3). (**F**) GsMTx4-treated NK cells exhibit enhanced capability of infiltration into collagen matrices. The NK cells were stained with CFSE and added on the top of solidified collagen matrices (2 mg/ml). The NK cells approached the bottom were visualized (left panel) and quantified (right panel).

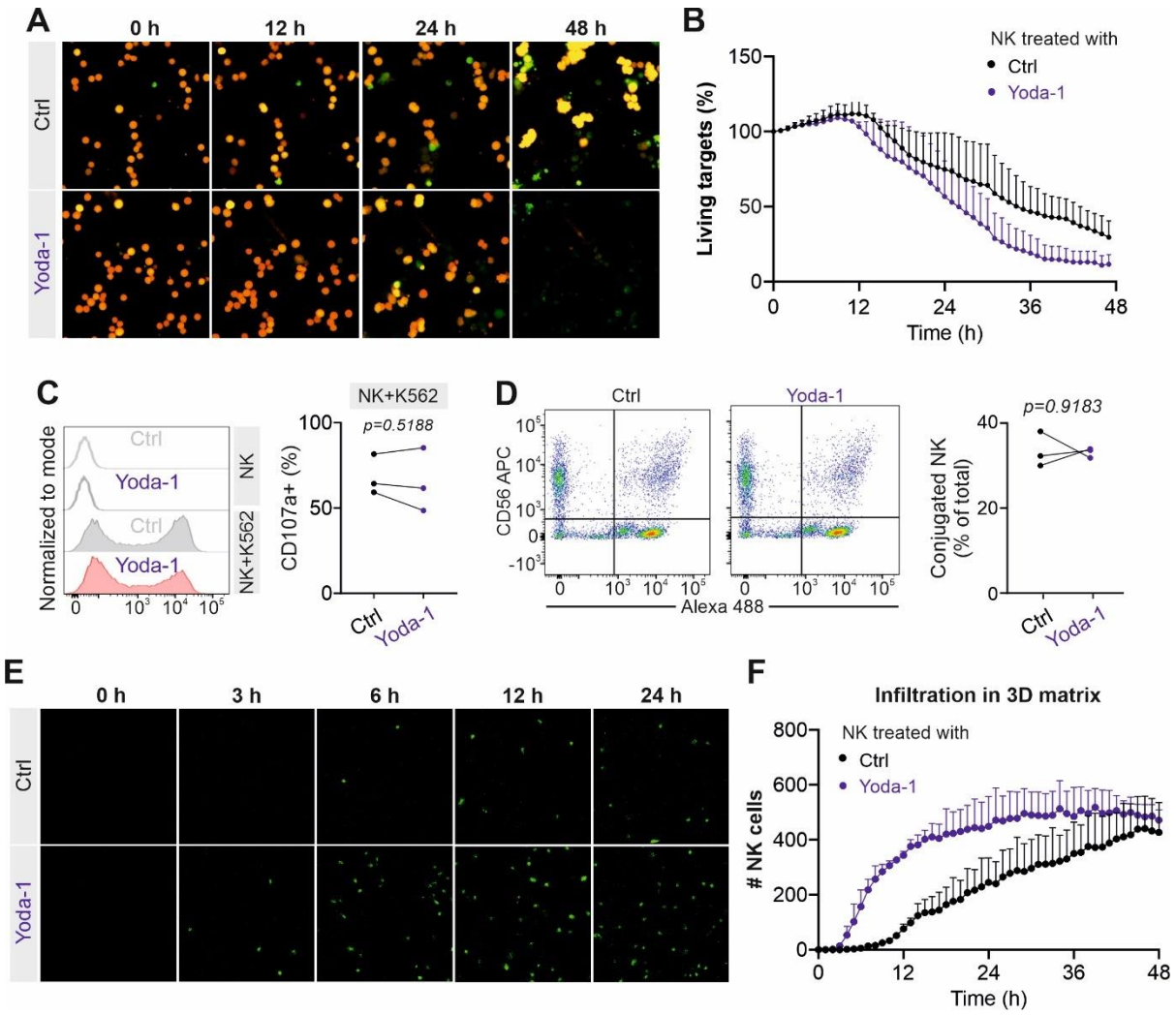

Figure 4. PIEZO1 activation enhances NK cell killing efficiency in 3D. Primary human NK cells from healthy donors were stimulated with IL-2 for three days. Prior to the experiments, the NK cells were pre-treated with Yoda-1 at 37°C for 30 minutes. Yoda-1 was present in the medium during the experiments. (**A-B**) Yoda-1 treatment enhances the killing efficiency of NK cells in 3D. K562-pCasper target cells were embedded in collagen matrices (2 mg/ml) and the NK cells were added from the top. Live target cells are in orange-yellow color and apoptotic target cells in green. Time lapse of one representative donor is shown in **A** and the quantification of all donors is shown in **B**. (**C-D**) GsMTx4 treatment does not affect degranulation and NK/target conjugation. NK cell degranulation induced by target cell recognition was evaluated using the CD107a degranulation assay (**C**, n=3). To evaluate NK/target conjugation, the NK cells were incubated with K562 target cells at 37°C for 30 minutes. Then the cell suspension was stained with anti-CD56 antibody to identify NK cells and K562 cells,

respectively. Double positive doublets were taken as NK/target conjugates and the analysis is shown in **D**. (**E-F**) NK infiltration into 3D collagen matrices is enhanced by Yoda-1 treatment. The NK cells were stained with CFSE and added on the top of solidified collagen matrices (2 mg/ml). The NK cells approached the bottom were visualized (**E**) and quantified (**F**).